ACS OMEGA

Open Access

http://pubs.acs.org/journal/acsodf

Article

Colorimetric Chitosan Films with Tunable Drug Release Ratio: Effect of Citric Acid and Acetic Acid Concentration Ratio and Drying Temperature

Hiroya Tsubota, Mai Horita, Akihiro Yabuki, Noriko Miyamoto, Sung Ho Jung,* and Ji Ha Lee*

Cite This: *ACS Omega* 2025, 10, 9088−9095

Read Online

ACCESS | Metrics & More | Article Recommendations | Supporting Information

ABSTRACT: This study successfully controlled the mechanical structure of chitosan films by regulating the interactions between chitosan molecules through variations in the concentration ratio of citric and acetic acids within the films. Additionally, precise drug release was achieved by adjusting the drying temperature during the synthesis. The key issue addressed is the challenge of achieving precise drug release control in biodegradable materials. Inaccurate drug release can lead to ineffective treatment or adverse side effects, limiting therapeutic efficacy and increasing healthcare challenges. The main objective was to fine-tune the films' composition and mechanical properties to achieve predictable control over drug release ratios. Our results show that increasing the concentration of citric acid enhanced the drug release ratio, while higher drying temperatures reduced the release ratio, likely due to structural changes in the film. Furthermore, structural changes in the chitosan films caused by varying the concentration ratio of citric acid to acetic acid enabled the successful control of the tensile strength and strain of the films. Additionally, we developed films capable of visually indicating the drug release ratio through color changes before and after release, providing a simple and effective method for real-time monitoring. Despite these promising results, challenges remain, such as improving the biocompatibility of films for use in complex biological environments. Future research will focus on enhancing durability, conducting further tests in biological systems, and exploring methods to increase the biocompatibility of films and their long-term performance.

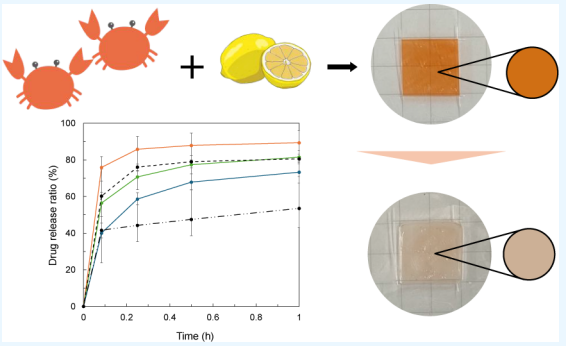

INTRODUCTION

Chitosan, a biopolymer derived from crustacean shells, is widely recognized for its exceptional biocompatibility and biodegradability.[1−3] These characteristics affirm its safety for human use and make it suitable for various biomedical applications,[4] including drug delivery systems and wound healing materials.[5,6] However, in drug delivery systems, challenges, such as systemic toxicity and navigation control, remain significant,[7,8] necessitating the development of more advanced and targeted delivery mechanisms. The biodegradability of chitosan ensures it decomposes into nontoxic products, which is essential for temporary implants and medical devices that require eventual breakdown in the body. Furthermore, chitosan offers a cost-effective and eco-friendly source of raw material, reinforcing its role as a sustainable option in medical biotechnology.[9] Kamat et al. have successfully developed a biocompatible drug delivery system using chitosan nanoparticles.[10] Moreover, there has been a concerted effort in recent years to enhance the properties of chitosan via chemical modification.[11−13] Sousa et al. have increased its antibacterial activity by modifying chitosan with phthalic anhydride and ethylenediamine.[14] However, modification of chitosan with potentially harmful substances could compromise its biocompatibility.

Chitosan films also enhance drug efficiency by enabling controlled release rates, which improve therapeutic outcomes and minimize dosing frequency.[15] Moreover, they can form protective barriers over wounds, delivering drugs while shielding against infection and aiding healing. In previous research, we successfully improved elasticity by adding acetic acid to chitosan.[16] Acetic acid has emerged as a notable modification material for chitosan.[17,18] Acetic acid, a monovalent carboxylic acid, is widely recognized as the primary component of vinegar.[19] However, the use of chitosan films is not without its challenges. A significant drawback is that drug release is dependent on concentration diffusion, which is difficult to control. As a solution to these issues, approaches that incorporate photoresponsive[20] or pH-

Received: September 9, 2024
Revised: January 28, 2025
Accepted: February 3, 2025
Published: February 26, 2025

responsive properties[21] into chitosan films to control drug release have been proposed. However, these methods often face challenges such as complex synthesis processes.

Building on previous research, we suggest a combination of citric acid and acetic acid as a modification material for chitosan. Citric acid, a trivalent carboxylic acid, is naturally abundant in various fruits and vegetables, particularly citrus fruits like lemons, limes, and grapefruits.[22] Moreover, citric acid is a vital compound supplied to the citric acid cycle in the body, serving as a significant energy source.[23] We hypothesize that using both citric and acetic acids will enhance the functionality of chitosan films, improving their drug delivery capabilities. By altering the concentration ratio of citric acid to acetic acid in chitosan films, the structure of the films can be controlled, enabling regulation of both drug release properties and mechanical characteristics. Additionally, the aim is to establish a drug delivery system using chitosan films that allows for visual confirmation of drug release.

MATERIALS AND METHODS

Materials. Chitosan (CS) solution (2 wt % slurry (water dispersion), n = 480) was obtained from Sugino Machine Ltd. Acetic acid (AA, MW = 60 g/mol) and doxorubicin hydrochloride (DOX) were purchased from TCI. Citric acid (CA, MW = 192.12 g/mol) and dimethyl sulfoxide (DMSO, >99.0%) were obtained from Wako Chemicals (Japan). These were used without further purification.

Preparation of CA_{3x}/CS Films at Different Concentration of Citric Acid. CS solution (2 wt %) of 500 mg was added to polypropylene ointment containers. Then, 32.34 μL of CA solution ranging 1 M, 2 M, and 5 M was added, followed by thorough mixing using a spatula to obtain CA_{3x}/CS solutions with varying concentrations [(i) $3x$ = 750, (ii) $3x$ = 1500, (iii) $3x$ = 3750, where x represents the relative amount of carboxyl groups]. The anticancer drug, DOX, was dissolved in DMSO to obtain an 8 mg/mL DOX solution. Twenty μL of the DOX solution was added to the various concentrations of CA_{3x}/CS solutions and mixed using a spatula to prepare DOX-loaded CA_{3x}/CS solutions. Subsequently, the DOX-loaded CA_{3x}/CS solutions were dried using an oven (OFW-300S, AS ONE Co., Ltd.) at temperatures of 40, 60, and 80 °C for 2 h each to obtain DOX-loaded CA_{3x}/CS films, respectively.

Preparation of $CA_{3x}AA_y$/CS Films at Different Mixture Ratio of Citric Acid and Acetic Acid. CS solution (2 wt %) of 500 mg was added to polypropylene ointment containers. Then, 16.17 μL of CA solution ranging from 4, 3.33, 2, 0.67, to 0, and 16.17 μL of AA solution ranging from 0, 2, 6, 10, to 12 M were added, followed by thorough mixing using a spatula to obtain $CA_{3x}AA_y$/CS solutions with varying $CA_{3x}AA_y$ ratios ((i) $3x$ = 1500, y = 0, (ii) $3x$ = 1250, y = 250, (iii) $3x$ = 750, y = 750, (iv) $3x$ = 250, y = 1250, (v) $3x$ = 0, y = 1500). These conditions ensured a constant number of carboxyl groups ($3x$ + y = 1500). A 20 μL portion of the DOX solution was added to the various $CA_{3x}AA_y$/CS solutions and mixed using a spatula to prepare DOX-loaded $CA_{3x}AA_y$/CS solutions. Subsequently, the DOX-loaded $CA_{3x}AA_y$/CS solutions were dried at a temperature of 40 °C for 2 h to obtain DOX-loaded $CA_{3x}AA_y$/CS films.

Drug Release Test. The drug release ratio from the CS films was measured using a UV−vis spectrophotometer (UV−vis, V-750, JASCO Corp.) in the range of 200 to 700 nm. A volume of 1.5 mL of phosphate buffer solution (PBS, 1.5 mL) was added to the ointment container containing the CS films at room temperature. For absorbance measurement, a sample (1.5 mL) was collected from the ointment container after a certain period, and then the solution was returned to the ointment container after each measurement. A quartz cell with a path length of 10 mm was used for the measurements. The drug release ratio was calculated using eq 1, where R_L is the amount of DOX encapsulated in the CS films and R_t is the amount of DOX released into 1.5 mL of PBS during each measurement period. The amount of released DOX was determined by using the calibration curve of DOX measured at a wavelength of 478.5 nm. The calibration curve used in this study is shown in Figure S1. All experiments were performed three times.

$$\text{Drug release ratio}(\%) = \frac{R_t}{R_L} \times 100 \tag{1}$$

FTIR Measurement. Following the same procedure described above, $CA_{3x}AA_y$/CS films were prepared, and the spectra were obtained using ATR-FTIR and acquired at a resolution of 4 cm^{-1} over the range of 400 to 4000 cm^{-1} by averaging 16 scans with an Agilent Cary 630 spectrometer equipped with a single reflection diamond crystal. The baseline was automatically corrected during the measurement.

Colorimetric Test. $CA_{3x}AA_y$/CS films, prepared following the same procedure described above, were cut into 10 × 10 mm^2 (length × width). Subsequently, 1.5 mL of PBS was added to an ointment container, and the container was left undisturbed for 1 h. The PBS solution adhering to the surface of the $CA_{3x}AA_y$/CS films was then removed using Kimwipes. The surface color of the $CA_{3x}AA_y$/CS films before and after swelling was observed. The CA3xAAy/CS films were photographed before and after swelling, and RGB was measured using the eyedropper tool in PowerPoint. The RGB was obtained by averaging the three points.

Kinetic Model for Analysis of the Drug Release Mechanisms. To analyze the drug release mechanism from the $CA_{3x}AA_y$/CS films, kinetic models were used. Zero-order (eq 2), first-order (eq 3), Higuchi (eq 4), and Korsmeyer−Peppas (eq 5) models were used. In eq 2−5, M_t represents the amount of drug released at distinct time points t, M_0 is the initial amount of drug in the release medium (in this case, M_0 = 0), R_0 is the initial drug release ratio in the release medium (in this case, R_0 = 0), K_0 and K_1 are the drug release constants for the Zero-order and first-order models respectively, K_H is the Higuchi constant, K_{KP} is the Korsmeyer−Peppas constant, M_t/M_∞ represents the fraction of drug released at distinct time points t, and n is the diffusion exponent.

$$M_t = M_0 + K_0 t \tag{2}$$

$$\log\left(100 - \frac{M_t}{M_\infty} \times 100\right) = \log\left(100 - \frac{M_0}{M_\infty} \times 100\right) - K_1 t \tag{3}$$

$$M_t = K_H t^{0.5} \tag{4}$$

$$\frac{M_t}{M_\infty} = K_{KP} t^n \tag{5}$$

Tensile Test. The tensile strength (TS) and elongation at break (EB) of the $CA_{3x}AA_y$/CS films were measured using a tensile strength tester (JSV-H1000, Japan Instrumentation System Co., Ltd.). $CA_{3x}AA_y$/CS films, prepared following the

https://doi.org/10.1021/acsomega.4c08272
ACS Omega 2025, 10, 9088−9095

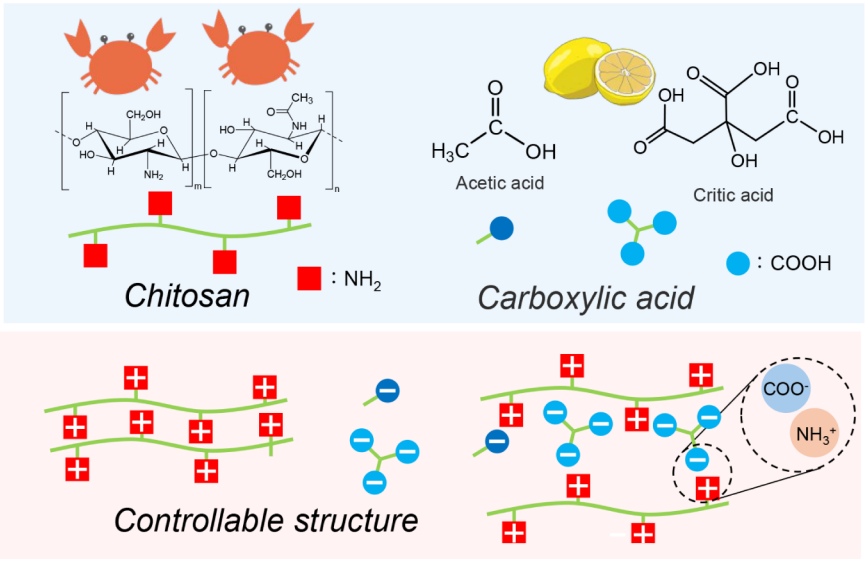

Figure 1. Mechanism of chitosan (CS) versus carboxylic acids of acetic acid (AA) and citric acid (CA).

same procedure described above, were cut into strips of 20 × 5 mm^2 (length × width). Both ends of the strips were attached to the analyzer with an initial grip spacing of 5 mm and were stretched at a speed of 5 mm/min. TS (MPa) and EB (%) were calculated using eqs 6 ,7 respectively. In eq 6, F represents the applied load (N), and A is the cross-sectional area (mm^2) of the $CA_{3x}AA_y$/CS film strip, calculated from the average thickness and width of the $CA_{3x}AA_y$/CS films. The average thickness of the $CA_{3x}AA_y$/CS films was determined by measuring three random points using an electromagnetic film thickness gauge (LE-200J, Kett Electric Laboratory), and then calculating the average value. In eq 7, L_0 is the initial length (mm) of the $CA_{3x}AA_y$/CS film strip, and L_1 is the final length (mm) of the $CA_{3x}AA_y$/CS film strip at the point of breakage. For each $CA_{3x}AA_y$/CS film, strain−stress curves were plotted, and the stretchability of the $CA_{3x}AA_y$/CS films was evaluated based on the elongation at the breakage point.

$$TS(\text{MPa}) = F/A \tag{6}$$

$$EB(\%) = (L_1 - L_0)/L_0 \times 100 \tag{7}$$

RESULTS AND DISCUSSION

The Effect of Citric Acid on Drug Release from DOX-loaded Chitosan Films at Different Drying Temperatures. The CS films loaded with DOX were prepared by adding DOX to solutions containing different component ratios of CA, AA, and CS. The reaction mechanism between CS and the carboxylic acids of weak acid is illustrated in Figure 1. The amine group of chitosan and the carboxylate of weak acid form an ionic bond between the two functional groups.

The conditions of the CA_{3x}/CS films are presented in Table 1, and the results of the drug release test using CA_{3x}/CS films are shown in Figure 2. For the CA_{3x}/CS films dried at 40 °C, films (a) and (d) exhibited a high drug release ratio of approximately 80%, while the CA_{3x}/CS film (g) dissolved during the test. For the CA_{3x}/CS films dried at 60 °C (b), (e), and (h), the drug release ratio of (b) and (e) is approximately 60%, and the CA_{3x}/CS film (h) dissolved. For the CA_{3x}/CS films dried at 80 °C (c), (f), and (i), the drug release ratio of (c) and (f) is approximately 10%, and the CA_{3x}/CS film (i) is approximately 60%. The drug release ratio of the CA_{3x}/CS films after 1 h plotted against the drying temperature, is shown in Figure S2. From these observations, it can be concluded that increasing the drying temperature results in a gradual decrease in the drug release ratio. This is likely influenced by the difference in drying rate during CA_{3x}/CS film synthesis.

Table 1. Synthesis Conditions of the CA/CS Films

Label	CA[M]	pH	Dry temperature [°C]	Average thickness (mm)
CA_{750}@40	1		40	0.207
CA_{750}@60	1	3.35	60	0.172
CA_{750}@80	1		80	0.136
CA_{1500}@40	2		40	0.207
CA_{1500}@60	2	3.40	60	0.103
CA_{1500}@80	2		80	0.120
CA_{3750}@40	5		40	0.231
CA_{3750}@60	5	2.79	60	0.219
CA_{3750}@80	5		80	0.204

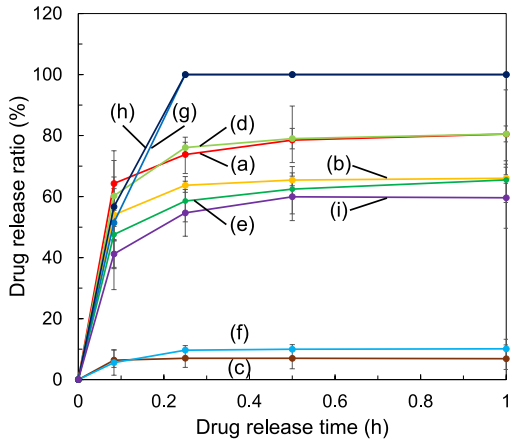

Figure 2. Drug release ratio at different concentrations of citric acid (CA): CA_{3x}/CS Films (a) CA_{750}@40, (b) CA_{750}@60, (c) CA_{750}@80, (d) CA_{1500}@40, (e) CA_{1500}@60, (f) CA_{1500}@80, (g) CA_{3750}@40, (h) CA_{3750}@60, and (i) CA_{3750}@80.

https://doi.org/10.1021/acsomega.4c08272
ACS Omega 2025, 10, 9088−9095

Figure 3 illustrates the mass change during the drying process of various CA_{3x}/CS films. Comparing the cases of

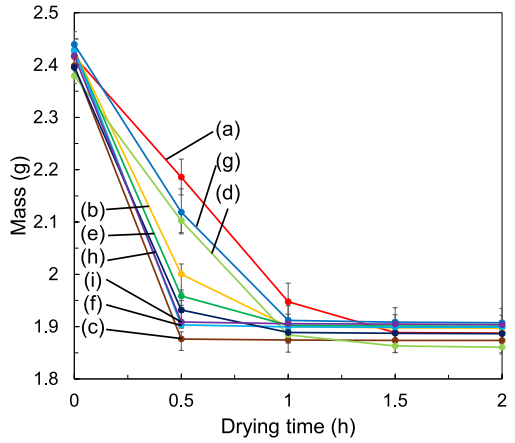

Figure 3. Mass variation during the drying process of CA_{3x}/CS films: (a) CA_{750}@40, (b) CA_{750}@60, (c) CA_{750}@80, (d) CA_{1500}@40, (e) CA_{1500}@60, (f) CA_{1500}@80, (g) CA_{3750}@40, (h) CA_{3750}@60, and (i) CA_{3750}@80.

drying temperatures at 40 and 80 °C from Figure 3, there is approximately a 2-fold difference in drying rate. According to a research report, the cross-section of CA_{3x}/CS films dried at high temperatures becomes denser and smoother compared to those dried at low temperatures, due to differences in crystalline structure and factors such as hydrogen bonding.[24] Therefore, in this experiment, it is conceivable that increasing the drying temperature resulted in a denser CA_{3x}/CS film structure, possibly suppressing drug release. Furthermore, from Figure 2, it is evident that varying the concentration of CA in the CA_{3x}/CS films leads to significant changes in the drug release ratio and water solubility of the CA_{3x}/CS films. CA_{3x}/CS films synthesized using solutions with a CA concentration of 5 M at drying temperatures of 40 and 60 °C (g,h) dissolved after 15 min. This is believed to be due to the decrease in chitosan interaction caused by the excessive addition of CA. Excessive addition of CA resulted in CA that did not bind to CS dissolving into the PBS. This caused a decrease in the pH of the PBS (Table S1), leading to the amino groups (NH_2 and $NH_3^+CH_3COO^-$) of CS becoming positively charged, resulting in strong repulsive forces between positive ions.[25] As a result, the network of the CA_{3x}/CS films expanded, leading to the collapse of CA_{3x}/CS films. The reason the CA_{3x}/CS film dried at 80 °C did not dissolve is believed to be that drying at 80 °C resulted in a denser CA_{3x}/CS film structure, making it difficult for CA to dissolve into the solvent, and the pH did not change significantly. Compared with the drug release ratio of the CS film without CA (Figure S3), adding CA to the CS film significantly enhances the drug release ratio. Additionally, CA_{250} and CA_{500} films were synthesized at room temperature, and their drug release test results are shown in Figure S4. The results indicate that CA_{750}@40 exhibited a higher drug release ratio. This suggests that the improvement in drug release by adding CA is more effective than that achieved by lowering the temperature. These results suggest that adjusting the drying temperature and CA concentration of CA_{3x}/CS films significantly influences their structure and drug release properties, highlighting the importance of selecting optimal conditions to achieve controlled drug release tailored to specific purposes.

The Effect of Citric Acid and Acetic Acid Mixture Ratios on Drug Release from DOX-loaded Chitosan Films. The synthesis conditions of $CA_{3x}AA_y$/CS films are presented in Table 2, and the mass change during the drying process of various $CA_{3x}AA_y$/CS films is shown in Figure S5, while the results of the drug release tests conducted using the synthesized $CA_{3x}AA_y$/CS films are shown in Figure 4. From

Table 2. Synthesis Conditions of $CA_{3x}AA_y$/CS Films

Label	CA [M]	AA [M]	pH	Average thickness (mm)
$CA_{1500}AA_0$	4	0	3.47	0.067
$CA_{1250}AA_{250}$	3.33	2	3.64	0.089
$CA_{750}AA_{750}$	2	6	3.83	0.132
$CA_{250}AA_{1250}$	0.67	10	4.10	0.072
CA_0AA_{1500}	0	12	5.12	0.109

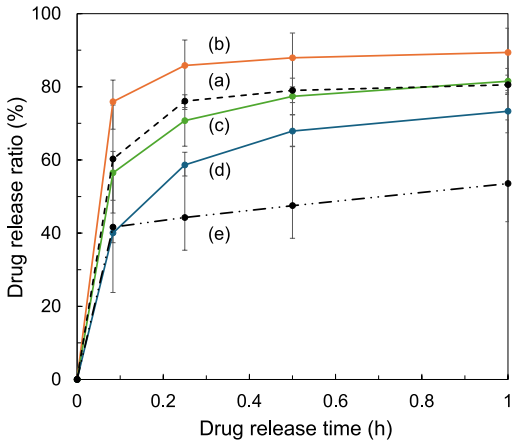

Figure 4. Drug release ratio at different mixture ratios of citric acid and acetic acid: $CA_{3x}AA_y$/CS Films (a) $CA_{1500}AA_0$, (b) $CA_{1250}AA_{250}$, (c) $CA_{750}AA_{750}$, (d) $CA_{250}AA_{1250}$, and (e) CA_0AA_{1500}.

Figure 4, it is evident that the drug release ratio varies with changes in the mixing ratio of CA and AA within the $CA_{3x}AA_y$/CS films. By altering the component ratios, we successfully achieved precise control over the drug release ratio, ranging from approximately 50% to 90%. The drug release ratio of each CA/CS film after 1 h is shown in Figure S6. In previous studies, the drug release ratio was controlled from 40% to 75% by adding AA to chitosan.[16] In this study, the drug release ratio was successfully controlled from 10% to 100% by adding AA and CA to chitosan and controlling the temperature of the drying process of the film. The range of drug release control in this study is superior compared to other drug delivery systems using chitosan.[26−28] As mentioned above, this is believed to be attributed to the decreased interaction between chitosan due to the presence of CA and AA. It is conceivable that the carboxyl groups (COO^-) of CA and AA form ion bonds with the amine groups ($NH3^+$) of CS, thereby strengthening the effect of hydrogen bonding. This likely results in a reduction of interactions among chitosan molecules, leading to the expansion of the CS network.[16] Moreover, under all conditions, the carboxyl groups derived from the carboxylic acids are present in equal amounts, but increasing the ratio of CA/AA leads to a higher drug release ratio. This is likely due to the difference in the pK_a values between CA and AA. The

https://doi.org/10.1021/acsomega.4c08272
ACS Omega 2025, 10, 9088−9095

pK_a values of CA are pK_{a1} = 3.12, pK_{a2} = 4.76, pK_{a3} = 6.39, while the pK_a value of AA is 4.75.[29] Therefore, as the pK_a of CA is smaller than that of AA, increasing the ratio of CA/AA results in a more acidic environment for the $CA_{3x}AA_y$/CS solution, potentially leading to a more significant expansion of the CS network through ion bonding. The pH measurements of each $CA_{3x}AA_y$/CS solution are presented in Table 2, where it can be observed that increasing the ratio of CA/AA results in a lower pH. These findings demonstrate that by adjusting the mixing ratio of CA and AA, as well as the drying process temperature, the drug release ratio of $CA_{3x}AA_y$/CS films can be precisely controlled, achieving a broader range of drug release control compared to other chitosan-based drug delivery systems, thus indicating the potential of this approach for more versatile and targeted drug release applications.

Drug Release Behavior Analysis of DOX-loaded Chitosan Films Using the Kinetics Model. To analyze the drug release behavior of CA_{3x}/CS films and $C_{A3x}AA_y$/CS films, various drug release models were employed, and the results are presented in Tables S2, S3 and 3. The coefficient of determination (R^2) values for the zero-order model ranged from 0.35 to 0.61, indicating a poor fit for all $CA_{3x}AA_y$/CS films. This is likely due to the zero-order model's assumption of a constant drug release rate.[30] Similarly, the R^2 values for the first-order model ranged from 0.52 to 0.76, also indicating a poor fit for all $CA_{3x}AA_y$/CS films. The first-order model typically describes the release behavior of water-soluble drugs, whereas the drug used in this study, DOX, is hydrophobic, contributing to the poor fitting.[31] Regarding the Higuchi model, only the $CA_{250}AA_{1250}$ film showed good fitting. This indicates that the drug release behavior from these $CA_{3x}AA_y$/CS films follows Fickian diffusion.[32] As for the Korsmeyer–Peppas model, increasing the ratio of CA resulted in smaller values of the diffusion coefficient (n). A smaller n value indicates that the swelling behavior of the $CA_{3x}AA_y$/CS films affects drug release.[33] As mentioned earlier, this could be attributed to the wider expansion of the CS network by increasing the concentration of CA. This analysis enables a deeper understanding of the underlying release mechanisms and guides the design of more effective drug delivery systems.

Table 3. Drug Release Kinetics Parameters

	Higuchi		Korsmeyer–Peppas		
	K	R^2	K	n	R^2
$CA_{1250}AA_{250}$	118.02	0.646	91.19	0.066	0.890
$CA_{750}AA_{750}$	80.11	0.663	84.07	0.150	0.958
$CA_{250}AA_{1250}$	88.46	0.872	77.52	0.247	0.950

Colorimetric Observations of DOX-loaded Chitosan Films Before and After Drug Release. Figure 5 shows images of $CA_{3x}AA_y$/CS films before and after drug release. From these images, it is evident that the color of the $CA_{3x}AA_y$/CS films changes significantly before and after drug release. Chitosan films without DOX and DOX alone do not change color when immersed in PBS (Figure S7). This change occurs due to the diffusion of DOX, which was initially loaded into the $CA_{3x}AA_y$/CS films, into PBS during the swelling process. The color changes of the $CA_{3x}AA_y$/CS films can be quantified using RGB color codes as follows: the $CA_{1500}AA_0$ film changes from (212, 112, 20) to (192, 168, 142), the $CA_{1250}AA_{250}$ film changes from (209, 106, 23) to (190, 154, 125), the $CA_{750}AA_{750}$ film changes from (199, 95, 19) to (205, 120, 71), the $CA_{250}AA_{1250}$ film changes from (207, 104, 17) to (186, 147, 119), and the CA_0AA_{1500} film changes from (202, 103, 29) to (191, 160, 139). The color change closely corresponds to the drug release profile shown in Figure 4. Therefore, it is possible to estimate the drug release ratio from the color change of the $CA_{3x}AA_y$/CS films. For instance, the $CA_{1500}AA_0$ film shows a color of (192, 168, 142) after drug release, indicating that when the $CA_{3x}AA_y$/CS film reaches this color, approximately 80% of the drug has been released. Similarly, color changes were observed for CACS films before and after drug release (Figure S8). These films represent a promising candidate for next-generation medical films, enabling visual monitoring of the drug release ratio.

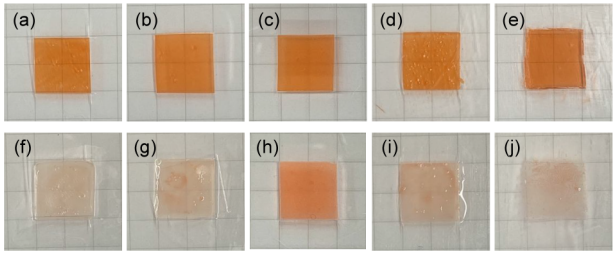

Figure 5. Photograph of $CA_{3x}AA_y$/CS Films at different mixture ratio of citric acid and acetic acid: (a) $CA_{1500}AA_0$, (b) $CA_{1250}AA_{250}$, (c) $CA_{750}AA_{750}$, (d) $CA_{250}AA_{1250}$, (e) CA_0AA_{1500}; and after drug release (f) $CA_{1500}AA_0$, (g) $CA_{1250}AA_{250}$, (h) $CA_{750}AA_{750}$, (i) $CA_{250}AA_{1250}$, and (j) CA_0AA_{1500}. "Photograph courtesy of 'Hiroya Tsubota'. Copyright 2024.".

FTIR Analysis of DOX-loaded Chitosan Films at Different Mixture Ratios of Citric Acid and Acetic Acid. The results of FTIR for the $CA_{3x}AA_y$/CS films before and after drug release are shown in Figure 6, and the FTIR results for DOX alone are shown in Figure S9. As shown in Figure S10, the peak corresponding to the amino groups of CS appears at 1590 cm^{-1}.[16] From Figure 6A, it can be observed that this peak shifts when CA and AA are added to CS. This shift is attributed to the reaction between the amino groups of CS and the carboxyl groups of CA and AA,[34] which aligns with the reaction mechanism depicted in Figure 1. Furthermore, by varying the ratio of CA and AA, fluctuations in the peaks at 1700 cm^{-1} originating from the C═O bond of the free carboxylic groups of CA[35] and at 1410 cm^{-1} originating from the COO^- stretching bonds of AA[36] could be confirmed. Figure 6 B presents the FTIR spectrum of the $CA_{3x}AA_y$/CS films after the drug release test, revealing a decrease in the peaks corresponding to CA and AA. This suggests that CA and AA are released from the $CA_{3x}AA_y$/CS films during the drug release process. After drug release, the overall sensitivity of the IR peaks decreased and the peaks became broader. This suggests that molecular bonding or structural changes occurred due to drug release. The release of DOX from the CS film likely weakened the hydrogen bonding between DOX and chitosan molecules, leading to these observed changes. The analysis of FTIR results for the $CA_{3x}AA_y$/CS films before and after drug release provides valuable insights into the molecular interactions and structural changes, shedding light on the release mechanism and the role of CA and AA in the drug delivery process.

Tensile Strength of DOX-loaded Chitosan Films at Different Mixture Ratios of Citric Acid and Acetic Acid. The results of the tensile tests on the $CA_{3x}AA_y$/CS films are presented in Figure 7. It can be observed that the mechanical

https://doi.org/10.1021/acsomega.4c08272
ACS Omega 2025, 10, 9088−9095

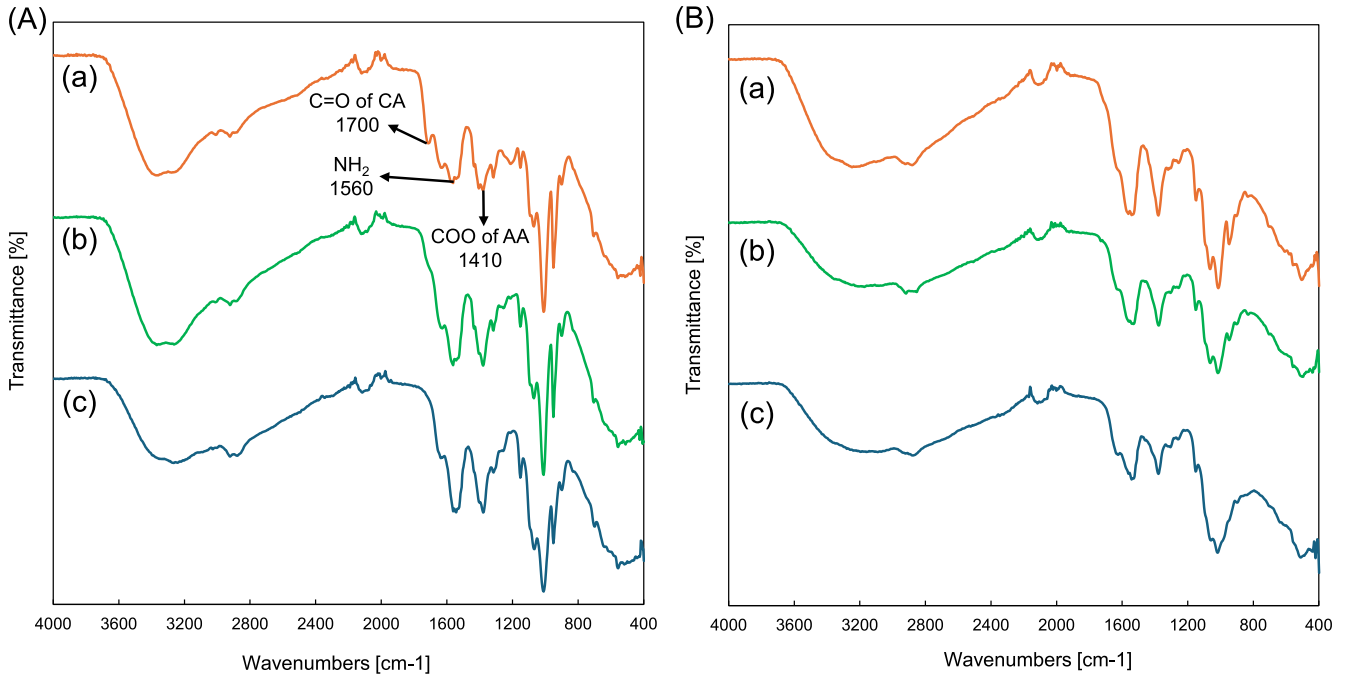

Figure 6. FTIR measurement of (A) before and (B) after drug release of $CA_{3x}AA_y$/CS films: (a) $CA_{1250}AA_{250}$, (b) $CA_{750}AA_{750}$, and (c) $CA_{250}AA_{1250}$.

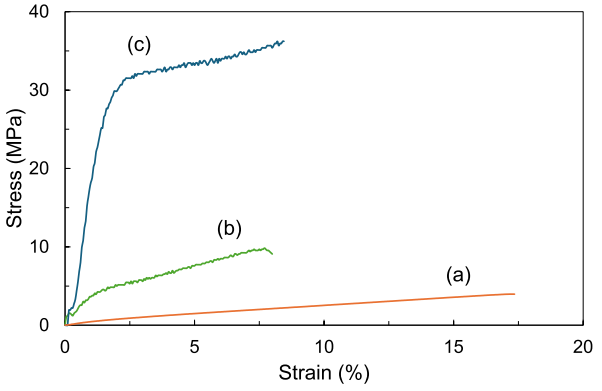

Figure 7. Tensile test of $CA_{3x}AA_y$/CS film: (a) $CA_{1250}AA_{250}$, (b) $CA_{750}AA_{750}$, (c) $CA_{250}AA_{1250}$.

properties of the $CA_{3x}AA_y$/CS films vary significantly by altering the mixing ratio of CA and AA in $CA_{3x}AA_y$/CS films. The $CA_{3x}AA_y$/CS film in (c) exhibited the highest tensile strength, approximately 36 MPa. Additionally, the elongation at the point of breakage of $CA_{3x}AA_y$/CS film (a) reached approximately 17%, indicating a remarkably high value. These results indicate that a higher AA concentration in the $CA_{3x}AA_y$/CS films enhances the tensile strength, while a higher CA concentration increases the elasticity. This may be due to the weakening of interactions between chitosan molecules as the CA concentration increases. Consequently, higher CA concentrations lead to increased elasticity but reduced tensile strength in $CA_{3x}AA_y$/CS films. Conversely, lowering the CA concentration reduces elasticity while enhancing tensile strength. Thus, by adjusting the mixing ratio of CA and AA appropriately, it is possible to control the mechanical properties of $CA_{3x}AA_y$/CS films.

CONCLUSION

The drying temperature during CS film synthesis significantly impacts the drug release ratio of the films, likely due to variations in drying speed affecting the film's structure. Additionally, the incorporation of citric acid (CA) and acetic acid (AA) influences the drug release ratio by altering the mechanical properties of the CS film. By carefully adjusting these factors, it is possible to synthesize CS films with finely controllable drug release ratios and mechanical properties. Additionally, the modification of chitosan films with citric and acetic acids was confirmed using FTIR, and it was also verified that changes in the concentration ratio of citric to acetic acid affect the control of the tensile strength and strain of the chitosan films. Furthermore, we successfully developed films capable of indicating the drug release percentage through color changes before and after the drug release. This ability to tailor the drug release profile and visually monitor the release percentage makes these films promising candidates for advanced medical applications. Our study findings have significant implications for controlled drug delivery systems, particularly in fields such as personalized medicine and localized treatment, where precise drug release can greatly improve patient outcomes and reduce side effects. By creating chitosan films that not only modulate drug release but also visually indicate release status, this work introduces a simple yet powerful tool for real-time therapeutic monitoring. Moreover, the biodegradable nature of chitosan makes this approach environmentally sustainable, potentially reducing the medical waste associated with traditional drug delivery devices. Therefore, further investigation into the biodegradability of chitosan films is expected to be necessary in the future.

ASSOCIATED CONTENT

Supporting Information

The Supporting Information is available free of charge at https://pubs.acs.org/doi/10.1021/acsomega.4c08272.

https://doi.org/10.1021/acsomega.4c08272
ACS Omega 2025, 10, 9088−9095

Standard curve of free DOX, drug release ratio at different drying temperature and different concentration of weak acid conditions, drug release kinetics parameter, photographs of before and after drug release of CS film, and FTIR of CS and DOX (PDF)

AUTHOR INFORMATION

Corresponding Authors

Sung Ho Jung − *Department of Chemistry, Research Institute of Advanced Chemistry, Gyeongsang National University, Jinju 52828, Republic of Korea;* orcid.org/0000-0002-5585-1086; Email: shjung@gnu.ac.kr

Ji Ha Lee − *Institute for Fiber Engineering and Science (IFES), Interdisciplinary Cluster for Cutting Edge Research (ICCER), Shinshu University, Ueda 386-8567, Japan;* orcid.org/0000-0002-4456-0128; Email: leejiha@shinshu-u.ac.jp

Authors

Hiroya Tsubota − *Chemical Engineering Program, Graduate School of Advanced Science and Engineering, Hiroshima University, Higashi-Hiroshima 739-8527, Japan*

Mai Horita − *Chemical Engineering Program, Graduate School of Advanced Science and Engineering, Hiroshima University, Higashi-Hiroshima 739-8527, Japan*

Akihiro Yabuki − *Chemical Engineering Program, Graduate School of Advanced Science and Engineering, Hiroshima University, Higashi-Hiroshima 739-8527, Japan*

Noriko Miyamoto − *Department of Materials Chemistry, Graduate School of Engineering, Aichi Institute of Technology, Toyota, Aichi 470-0392, Japan*

Complete contact information is available at: https://pubs.acs.org/10.1021/acsomega.4c08272

Author Contributions

The manuscript was written with contributions from all authors. All authors have given approval to the final version of the manuscript.

Notes

The authors declare no competing financial interest.

ACKNOWLEDGMENTS

This research was supported by the National Research Foundation of Korea (NRF) grant funded by the Korean government (MSIT) (RS-2023-00241926).

REFERENCES

(1) Adeyemi, A. O.; Ojoawo, S. O. Production and Characterization of Chitosan of Crustacean Shells. *Mater. Today: proc.* **2023**, *88*, 128−134.

(2) Harugade, A.; Sherje, A. P.; Pethe, A. Chitosan: A Review on Properties, Biological Activities and Recent Progress in Biomedical Applications. *React. Funct. Polym.* **2023**, *191*, 105634.

(3) Hisham, F.; Maziati Akmal, M. H.; Ahmad, F.; Ahmad, K.; Samat, N. Biopolymer Chitosan: Potential Sources, Extraction Methods, and Emerging Applications. *Ain Shams Eng. J.* **2024**, *15*, 102424.

(4) Devi, N. A.; Jegatheesan, A.; Raj, M. S. A.; Sundari, M. M.; Kajli, S. K.; Srinivasan, K.; Ravikumar, P.; Ayyanar, M.; Ravichandran, K.; Varshini, M.; Mohan, R. Cost-Effective Synthesis of Zinc Oxide/Crab Shell-Derived Chitosan Nanocomposite: Insights into Its Biomedical Applications. *Int. J. Biol. Macromol.* **2024**, *283*, 137869.

(5) Demir, D.; Ceylan, S.; Bölgen, N. Chitosan Based Injectable Cryospheres as a Potential Biopolymeric Carrier for Drug Delivery Systems: Characterization, Biocompatibility and Drug Release. *J. Drug Deliv. Sci. Technol.* **2024**, *102*, 106406.

(6) Naghib, S. M.; Hosseini, S. N.; Beigi, A. 3D/4D Printing of Chitosan-Based Materials for Wound Healing with Chitosan-Based Materials, Which Provide a Fresh Method for Creating Customized Scaffolds and Wound Dressings Applications. *Carbohydr. Polym. Technol. Appl.* **2024**, *8*, 100594.

(7) Lim, Y. Y.; Zaidi, A. M. A.; Miskon, A. Composing On-Program Triggers and On-Demand Stimuli into Biosensor Drug Carriers in Drug Delivery Systems for Programmable Arthritis Therapy. *Pharmaceuticals* **2022**, *15*, 1330.

(8) Lim, Y. Y.; Miskon, A.; Zaidi, A. M. A. CuZn Complex Used in Electrical Biosensors for Drug Delivery Systems. *Materials* **2022**, *15* (21), 7672.

(9) Ul-Islam, M.; Alabbosh, K. F.; Manan, S.; Khan, S.; Ahmad, F.; Ullah, M. W. Chitosan-Based Nanostructured Biomaterials: Synthesis, Properties, and Biomedical Applications. *Adv. Ind. Eng. Polym. Res.* **2024**, *7*, 79−99.

(10) Kamat, V.; Marathe, I.; Ghormade, V.; Bodas, D.; Paknikar, K. Synthesis of Monodisperse Chitosan Nanoparticles and in Situ Drug Loading Using Active Microreactor. *ACS Appl. Mater. Interfaces* **2015**, *7* (41), 22839−22847.

(11) Garreau, C.; Chiappisi, L.; Micciulla, S.; Morfin, I.; Trombotto, S.; Delair, T.; Sudre, G. Preparation of Highly Stable and Ultrasmooth Chemically Grafted Thin Films of Chitosan. *Soft Matter* **2023**, *19* (8), 1606−1616.

(12) Torkaman, S.; Najafi, S. H. M.; Ashori, A.; Mohseni, F. A. Chemoselective Modification of Chitosan with Arginine and Hydroxyproline: Development of Antibacterial Composite Films for Wound Healing Applications. *Int. J. Biol. Macromol.* **2024**, *282* (Pt 3), 137081.

(13) Zhang, B.; Zhou, J.; Li, Y.; Chen, J.; Zhang, Y. Bioactive Modification of Cyclic Olefin Copolymer (COC) Film Surfaces by Hyaluronic Acid and Chitosan for Enhanced Cell Adhesion. *Int. J. Biol. Macromol.* **2024**, *281*, 136169.

(14) Sousa, J. M.; Braz, E. M. A.; Bezerra, R. D. S.; Morais, A. I. S.; Vieira, A. C. C.; Costa, M. P.; Rizzo, M. S.; Chaves, L. L.; Barreto, H. M.; Osajima, J. A.; et al. Study of the Antibacterial and Cytotoxic Activity of Chitosan and Its Derivatives Chemically Modified with Phthalic Anhydride and Ethylenediamine. *Int. J. Biol. Macromol.* **2024**, *263*, 130292.

(15) Desai, N.; Rana, D.; Salave, S.; Gupta, R.; Patel, P.; Karunakaran, B.; Sharma, A.; Giri, J.; Benival, D.; Kommineni, N. Chitosan: A Potential Biopolymer in Drug Delivery and Biomedical Applications. *Pharmaceutics* **2023**, *15*, 1313.

(16) Lee, J. H.; Tachibana, T.; Wadamori, H.; Yamana, K.; Kawasaki, R.; Kawamura, S.; Isozaki, H.; Sakuragi, M.; Akiba, I.; Yabuki, A. Drug-Loaded Biocompatible Chitosan Polymeric Films with Both Stretchability and Controlled Release for Drug Delivery. *ACS Omega* **2023**, *8*, 1282.

(17) Bai, R.-K.; Huang, M.-Y.; Jiang, Y.-Y. Selective Permeabilities Of Chitosan-Acetic Acid Complex Membrane And Chitosan-Polymer Complex Membranes For Oxygen And Carbon Dioxide. *Polym. Bull.* **1988**, *20*, 83−88.

(18) Kou, S.; Peters, L. M.; Mucalo, M. R. Chitosan: A Review of Sources and Preparation Methods. *Int. J. Biol. Macromol.* **2021**, *169*, 85−94.

(19) Wang, D.; Feng, D.; Zhong, Q.; An, H.; Wu, Z.; Zhang, Q.; Yue, H.; Hu, L.; Liu, Y.; Wang, X.; et al. A New Method to Analysis Synthetic Acetic Acid to Vinegar: Hydrogen Isotope Ratio at the Methyl Site of Acetic Acid in Vinegar by GC-IRMS. *Food Chem.* **2024**, *451*, 139443.

(20) Naghib, S. M.; Amiri, S.; Mozafari, M. R. Stimuli-Responsive Chitosan-Based Nanocarriers for Drug Delivery in Wound Dressing Applications: A Review. *Carbohydr. Polym. Technol. Appl.* **2024**, *7*, 100497.

(21) Tian, B.; Liu, J. Smart Stimuli-Responsive Chitosan Hydrogel for Drug Delivery: A Review. *Int. J. Biol. Macro.* **2023**, *235*, 123902.

https://doi.org/10.1021/acsomega.4c08272
ACS Omega 2025, 10, 9088−9095

(22) He, J.; Sun, J.; Huang, Y.; Wang, L.; Liu, S.; Jiang, Z.; Wang, X.; Xu, Q. Transcriptome Analysis Reveals the Common and Specific Pathways of Citric Acid Accumulation in Different Citrus Species. *Hortic. Plant J.* **2024**.
(23) Roosterman, D.; Cottrell, G. S. Discovery of a Second Citric Acid Cycle Complex. *Heliyon* **2023**, *9* (5), No. e15968.
(24) Liu, F.; Chang, W.; Chen, M.; Xu, F.; Ma, J.; Zhong, F. Tailoring Physicochemical Properties of Chitosan Films and Their Protective Effects on Meat by Varying Drying Temperature. *Carbohydr. Polym.* **2019**, *212*, 150−159.
(25) Che, Y.; Li, D.; Liu, Y.; Ma, Q.; Tan, Y.; Yue, Q.; Meng, F. Physically Cross-Linked PH-Responsive Chitosan-Based Hydrogels with Enhanced Mechanical Performance for Controlled Drug Delivery. *RSC Adv.* **2016**, *6* (107), 106035−106045.
(26) Radha, D.; Lal, J. S.; Devaky, K. S. Release Studies of the Anticancer Drug 5-Fluorouracil from Chitosan-Banana Peel Extract Films. *Int. J. Biol. Macromol.* **2024**, *256* (Pt 2), 128460.
(27) Soares, Í.; Faria, J.; Marques, A.; Ribeiro, I. A. C.; Baleizão, C.; Bettencourt, A.; Ferreira, I. M. M.; Baptista, A. C. Drug Delivery from PCL/Chitosan Multilayer Coatings for Metallic Implants. *ACS Omega* **2022**, *7* (27), 23096−23106.
(28) Cardoso, H. P.; Bacalhau Rodrigues, J. F.; Nunes da Silva, H.; Galdino, T. P.; Luna, C. B. B.; Fook, M. V. L.; Montazerian, M.; Baino, F.; de Lima Silva, S. M. Chitosan/Montmorillonite Nanocomposite Film as Anticancer Drug Carrier: A Promising Biomaterial to Treat Skin Cancers. *Ceram. Int.* **2024**, *50* (11), 18528−18539.
(29) Mazinanian, N.; Odnevall Wallinder, I.; Hedberg, Y. Comparison of the Influence of Citric Acid and Acetic Acid as Simulant for Acidic Food on the Release of Alloy Constituents from Stainless Steel AISI 201. *J. Food Eng.* **2015**, *145*, 51−63.
(30) Zhao, Y. N.; Gu, J.; Jia, S.; Guan, Y.; Zhang, Y. Zero-Order Release of Polyphenolic Drugs from Dynamic, Hydrogen-Bonded LBL Films. *Soft Matter* **2016**, *12* (4), 1085−1092.
(31) Rakib Hasan Khan, M.; Shankar Hazra, R.; Nair, G.; Mohammad, J.; Jiang, L.; Reindl, K.; Khalid Jawed, M.; Ganai, S.; Quadir, M. Cellulose Nanofibers as Scaffold-Forming Materials for Thin Film Drug Delivery Systems. *Int. J. Pharm.* **2022**, *627*, 122189.
(32) Cabrera-Barjas, G.; Becherán, L.; Valdés, O.; Giordano, A.; Segura-Del Río, R.; Bravo-Arrepol, G.; Durán-Lara, E. F.; Cea, J.; Berg, A.; Castaño A, J.; Rodríguez-Llamazares, S.; Fuentes, G.; Katsarov, P.; Lukova, P.; Delattre, C. Effect of Cellulose Nanofibrils on Vancomycin Drug Release from Chitosan Nanocomposite Films. *Eur. Polym. J.* **2023**, *197*, 112371.
(33) Altunkaynak, F.; Okur, M.; Saracoglu, N. Controlled Release of Paroxetine from Chitosan/Montmorillonite Composite Films. *J. Drug Deliv. Sci. Technol.* **2022**, *68*, 103099.
(34) Ghosh, A.; Ali, M. A. Studies on Physicochemical Characteristics of Chitosan Derivatives with Dicarboxylic Acids. *J. Mater. Sci.* **2012**, *47* (3), 1196−1204.
(35) Loukri, A.; Kyriakoudi, A.; Oliinychenko, Y.; Stratakos, A. C.; Lazaridou, A.; Mourtzinos, I. Preparation and Characterization of Chitosan-Citric Acid Edible Films Loaded with Cornelian Cherry Pomace Extract as Active Packaging Materials. *Food Hydrocoll* **2024**, *150*, 109687.
(36) Sikorski, D.; Bauer, M.; Frączyk, J.; Draczyński, Z. Antibacterial and Antifungal Properties of Modified Chitosan Nonwovens. *Polymers* **2022**, *14* (9), 1690.

https://doi.org/10.1021/acsomega.4c08272
ACS Omega 2025, 10, 9088−9095